

Optimising the flow within a Stirling pulse tube cryocooler

M. A. Abolghasemi*, K. Liang**, R. Stone* , M. Dadd* and P. Bailey*
Corresponding author: amin.abolghasemi@eng.ox.ac.uk

* Department of Engineering Science, University of Oxford, UK

** Department of Engineering and Design, University of Sussex, UK.

Abstract: One of the key requirements for successful operation of Stirling pulse tube cryocoolers is to minimise flow mixing within the pulse tube. This requires careful design of the inlet and outlet to the pulse tube. In this study, the flow within the pulse tube of an existing cryocooler is numerically analysed. Thereafter, alternative inlet/outlet designs are suggested and analysed in order to optimise the flow within the pulse tube cryocooler. The numerical simulation have been carried out using CONVERGE CFD, a finite volume Navier-Stokes solver. The standard $k - \epsilon$ RANS turbulence model has been used to account for the effects of turbulence within the pulse tube.

Keywords: Computational Fluid Dynamics, Turbulence Modelling, Porous media, Heat transfer.

1 Introduction

Stirling pulse tube cryocoolers (SPTCs) are small low temperature refrigerators that can provide cooling for electronic devices such as infra-red sensors and superconducting devices. The pulse tube within an SPTC acts as a gas spring and replaces the cold end displacer used in traditional Stirling cryocoolers. Hence, there are no moving parts in the cold head assembly of an SPTC. This is a significant advantage from a design and manufacturing point of view. However, in order to ensure successful operation the gas within the pulse tube of an SPTC needs to remain stratified and flow mixing must be minimised. Hence, the inlet and outlet to the pulse tube must be designed with great care.

Fig. 1 shows a schematic of a typical in-line SPTC arrangement. The assembly consists of:

- An oil free linear compressor which generates a pressure wave.
- A regenerator which is typically filled with fine stainless steel wire mesh (REG in Fig. 1). The working fluid (usually Helium) exchanges heat with the regenerator material and a temperature profile develops along the regenerator.
- A cold end heat exchanger which is filled with copper wire mesh and acts as a heat sink (CHX in Fig. 1). This is where the lowest temperature is observed.
- A pulse tube which transfers enthalpy from the warm end to the cold end (PT in Fig. 1).
- A warm end heat exchanger at ambient temperature which is also filled with copper wire mesh (WHX in Fig. 1).
- A phase control mechanism which can either consist of a long inertance tube and a reservoir [1, 2, 3] or a phase shifter [4, 5, 6]. This is used to ensure the correct relationship between mass flow and pressure pulse at the cold end.

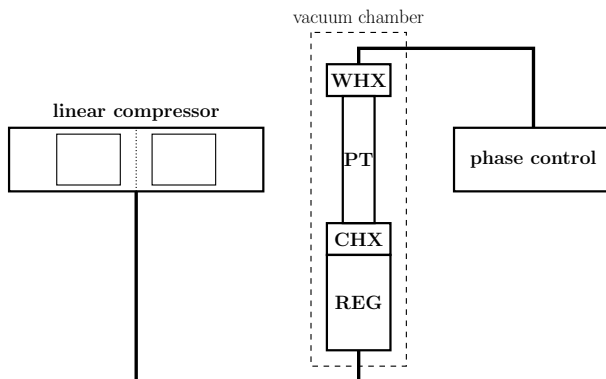


Figure 1: In-line SPTC schematic with abbreviations **REG** for *regenerator*, **PT** for *pulse tube*, **CHX** for *cold end heat exchanger* and **WHX** for *warm end heat exchanger*.

- A vacuum chamber is used to house the cold head assembly, consisting of the regenerator and the pulse tube. This is in order to minimise convective losses.

The heat exchangers either side of the pulse tube are also designed to act as flow straighteners. This is because a uniform flow profile is desired upon entry to the pulse tube as this will help maintain a stratified profile. However, these flow straighteners will introduce additional pressure drops which should be kept to a minimum as a significant pressure drop will have an adverse effect on the overall SPTC efficiency.

This study focuses on the design of suitable flow straighteners that minimise flow mixing inside the pulse tube without introducing significant pressure drops. The focus will be on the warm end heat exchanger as this will be easier to change in an experimental setup. Initially, the flow within an existing in-line SPTC design is numerically examined. Thereafter, two alternative flow straightener designs are suggested and each is assessed numerically. By examining the flow and pressure drops across all three designs, a suitable flow straightener design is selected. Experimental validations of the numerical work presented here will be carried out in future studies.

2 Methodology

Fig. 2 shows a simplified drawing of the pulse tube (including the heat exchangers at either end) of an existing design. This is based on the in-line SPTC developed at the Cryogenic Engineering Group at the University of Oxford. This SPTC has a typical operating frequency of around 60 Hz and a fill pressure of 28 bar. It has a thin walled stainless steel pulse tube with an internal diameter of 7.7 mm and a height of 85 mm. The heat exchangers (i.e. flow straighteners) have an internal diameter of 13 mm and a height of 5.5 mm. They are filled with copper 50-mesh (wires per inch). During operation, the cold end is maintained at 80 K and the warm end is kept at ambient.

2.1 Numerical model

The rotational symmetry of the pulse tube geometry meant that a 2D axis-symmetric model could be used for the numerical simulations. The simulations were carried out using CONVERGE CFD [7], a finite volume Navier-Stokes solver with adaptive mesh refinement capabilities. A sinusoidal velocity, u_{WHX} , was prescribed at the inlet to the warm end

$$u_{\text{WHX}} = 31.7 \sin(2\pi ft) \quad \text{m/s}, \quad (1)$$

with operating frequency f set to 60 Hz and where t is time passed in seconds. This was based on a peak-to-peak mass flow variation of 0.7 g/s at the warm end.

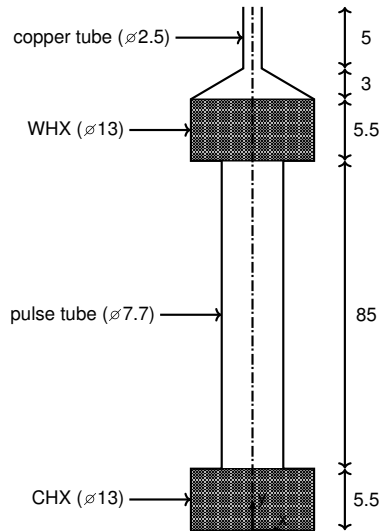


Figure 2: A simplified drawing of an in-line SPTC. All dimensions are in millimeters. Not drawn to scale. This will be referred to as **design A**.

Similarly, a sinusoidal pressure, P_{CHX} , was prescribed at the cold end

$$P_{\text{CHX}} = 28 + 3 \sin(2\pi ft + 4\pi/3) \quad \text{bar}, \quad (2)$$

where a peak-to-peak variation of 6 bar and a phase difference of $4\pi/3$ was assumed. The temperatures at the top and bottom boundaries were fixed at 300 K and 80 K, respectively. All other external boundaries were assumed to be adiabatic. Furthermore, the standard $k - \varepsilon$ RANS turbulence model was used to account for the effects of turbulence within the pulse tube. In order to establish cyclic steady state, the numerical simulations were run for 20 cycles.

The numerical grid used in the simulations for design A is shown in Fig. 3. A regular grid has been used with a finer resolution in the pulse tube and at the warm end inlet where the velocities are expected to be higher.



Figure 3: Numerical grid used for design A.

2.2 Alternative designs

Two alternative designs for WHX were suggested. The focus was on removing the abrupt change in cross section from WHX to the pulse tube in design A (Fig. 2). The modifications needed to be simple and easy to implement. The two designs are shown in Fig. 4. In design B, the cross-sectional diameter is simply reduced to match that of the pulse tube. In design C, a tapered WHX is used to gradually reduce the diameter from 13 mm to 7.7 mm without changing the overall assembly height.

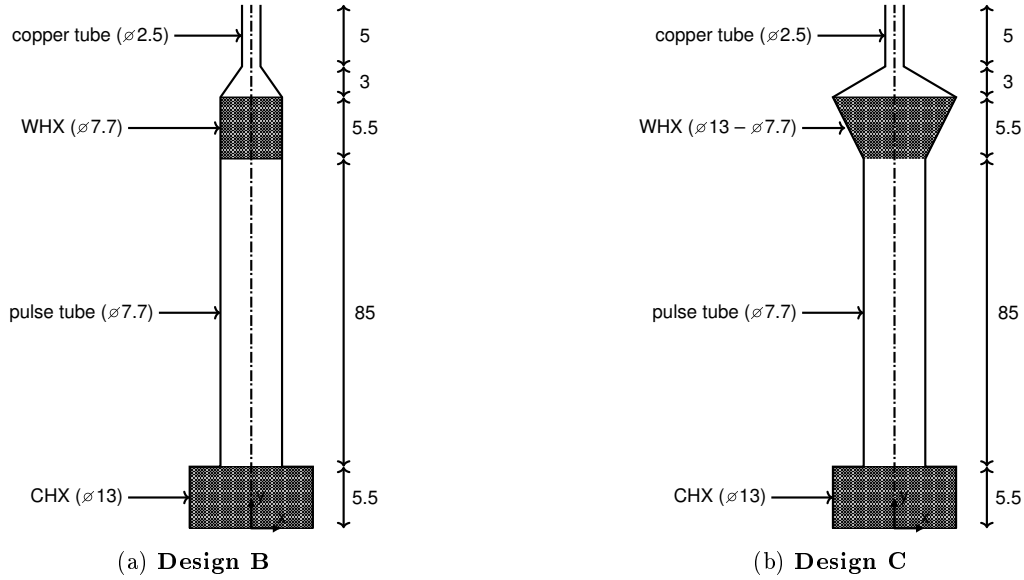


Figure 4: Alternative designs for the warm end heat exchanger. All dimensions are in millimeters. Not drawn to scale.

3 Results

3.1 Velocity

The velocity magnitude during maximum flow from the warm end (WHX) to the cold end (CHX) and vice versa are shown in Fig. 5–6. The velocity within all three inlet designs is similar, except for the region within the pulse tube closest to WHX. When flowing from WHX to CHX, the current inlet design (i.e. design A) leads to the greatest mixing (see Fig. 5a), while design B leads to the most uniform profile (see Fig. 5b). Design C is an improvement on design A, but does not perform as well as design B (see Fig. 5c). When flowing in the opposite direction from CHX to WHX, all three appear very similar apart from small differences very close to WHX (see Fig. 6). It is worth pointing out that the non-uniform behaviour near CHX suggests that there is room for improvement on the design of CHX as well.

In order to look at the differences in greater detail, velocity profiles at three different location along the pulse tube are shown in Fig. 7 (flowing WHX to CHX) and Fig. 8 (flowing CHX to WHX). When flowing from WHX to CHX, the greatest difference between the three designs occurs close to WHX (see Fig. 7a). Here the sharp change in cross section in design A leads to a higher velocity flow region near the pulse tube wall. On the other hand, reducing the WHX diameter in design B has helped avoid this and leads to a fairly uniform profile. In design C, the high velocity region is still present but its effect has been reduced. Having said that, non-uniform profiles of designs A and C do not last long and all three designs lead to fairly uniform profiles from the middle of the pulse tube onwards (see Fig. 7b–7c).

When flowing from CHX to WHX, all three designs lead to very similar velocity profiles. This is because the main factor in the development of the flow here is the shape of CHX which is the same for all three designs. The non-uniform profiles observed in Fig. 8c suggests that the design of CHX also needs to be altered in the future in order to ensure a more uniform profile.

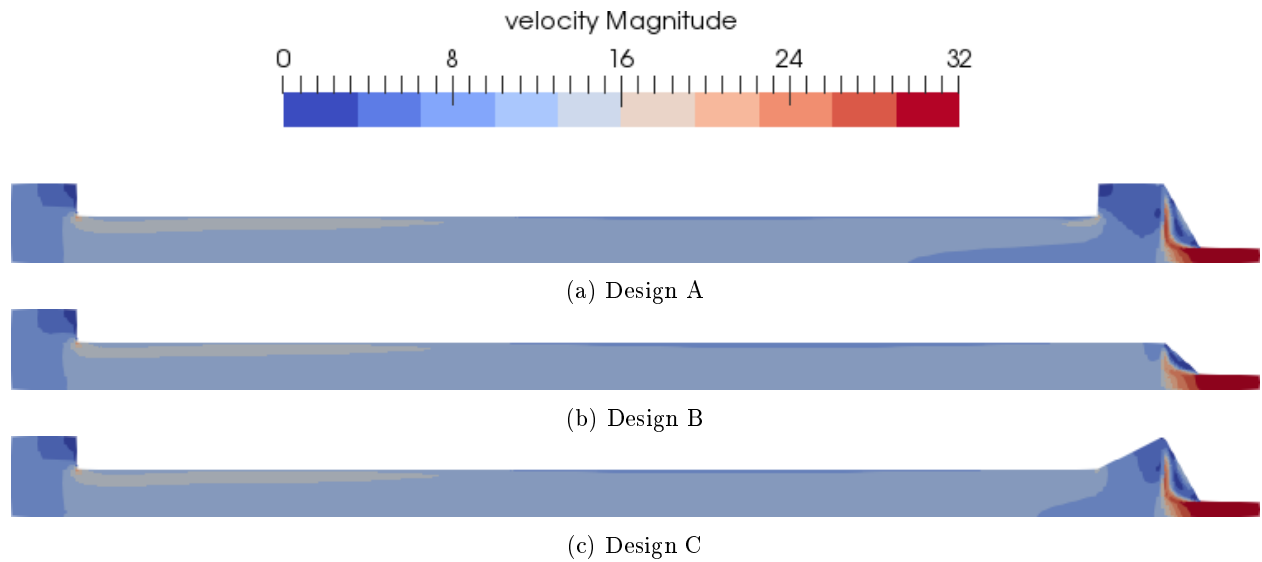


Figure 5: Velocity magnitude during maximum flow from WHX to CHX.

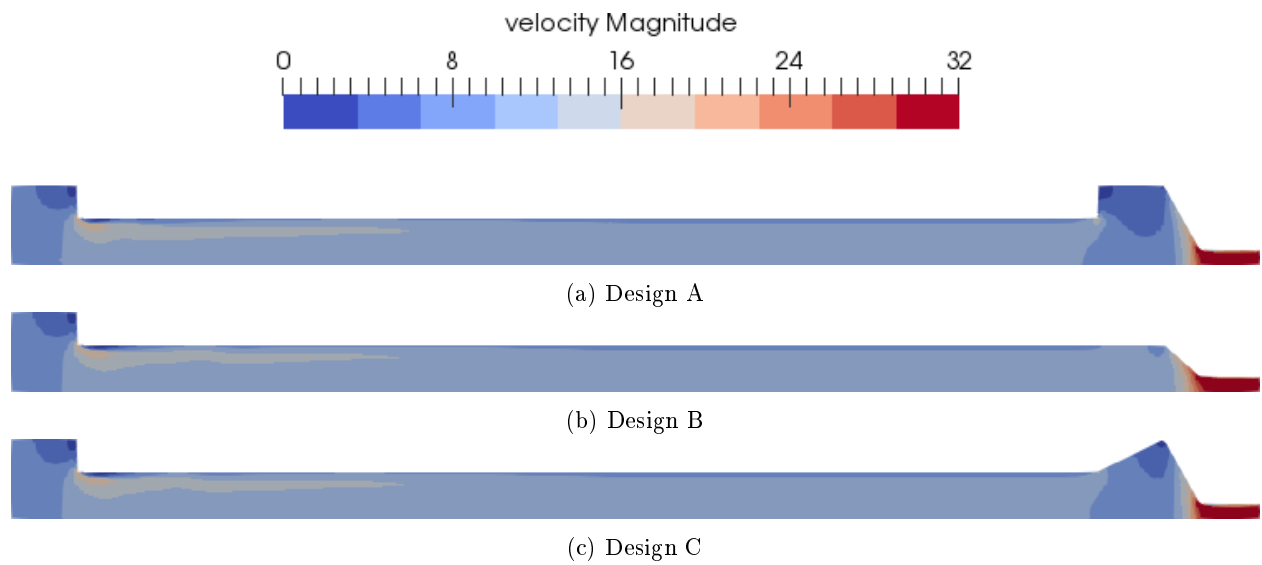


Figure 6: Velocity magnitude during maximum flow from CHX to WHX.

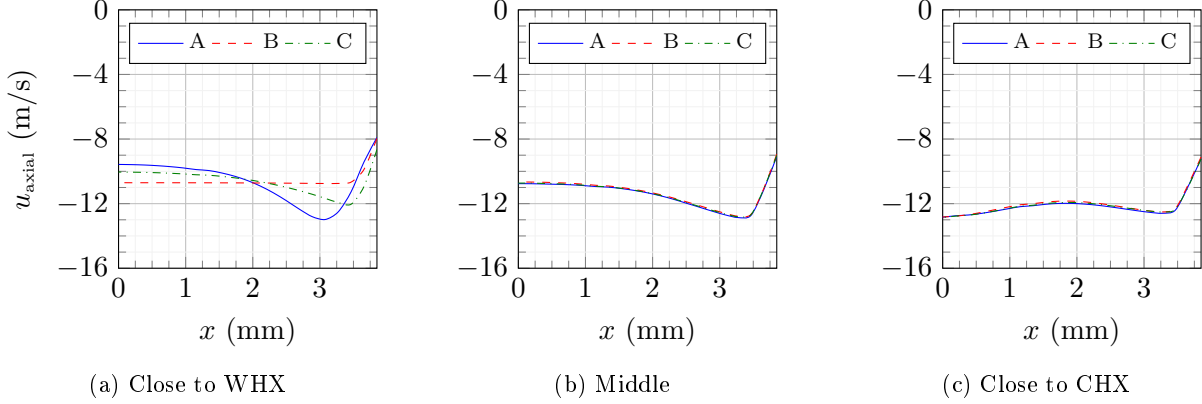


Figure 7: Cross-section velocity profiles at three different locations along the pulse tube during maximum flow (WHX to CHX).

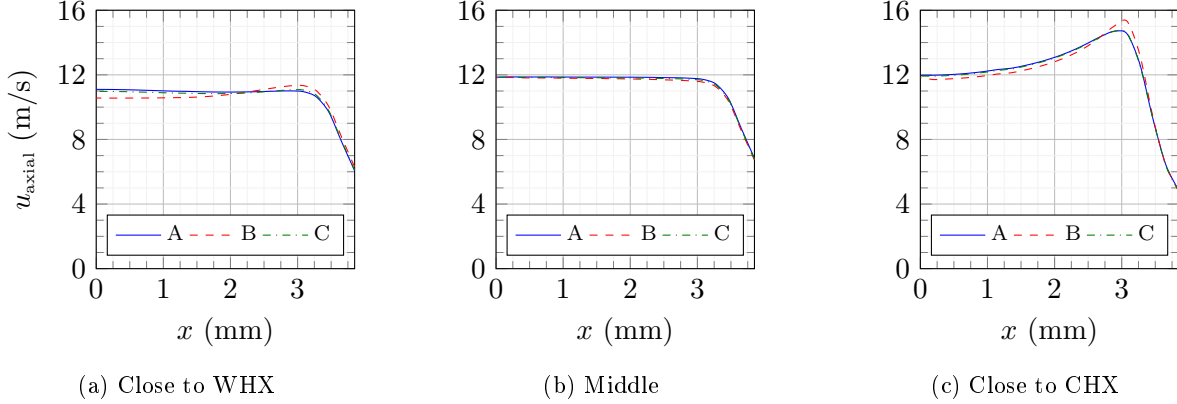
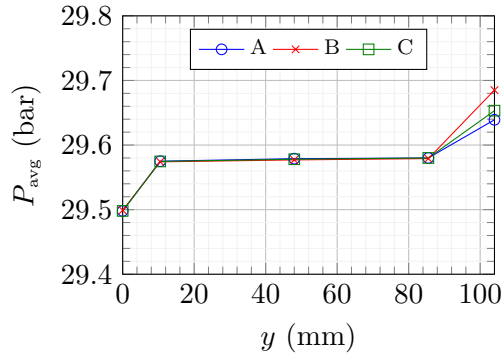


Figure 8: Cross-section velocity profiles at three different locations along the pulse tube during maximum flow (CHX to WHX).

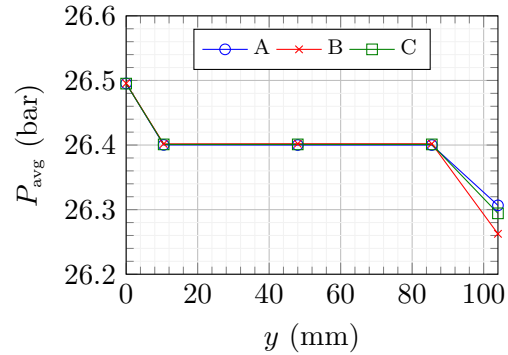
3.2 Averaged pressure

Based on the velocity profiles, design B is the clear favourite. However, the reduced cross-section in design B will lead to a greater pressure drop across WHX. In order to examine this in detail, the averaged pressures at various locations along the pulse tube for all three designs were calculated and the results are shown in Fig. 9. Based on the results shown, the pressure drop across WHX increases from 59 mbar in design A to 105 mbar in design B when flowing from WHX to CHX. When flowing from CHX to WHX it increases from 93 mbar in design A to 138 mbar in design B. On the other hand, design C leads to a marginal increase in pressure drop compared to design A.

The increase in pressure drop in design B is by no means insignificant, however given that the peak-to-peak variation in pressure within the SPTC is of the order of a few bars, an increase in pressure drop in the order of 10 mbar might not have a significant effect on the overall cryocooler efficiency. In order to be able to quantify this, experiments need to be carried out to see if the advantages of the uniform flow in design B outweigh the potential drop in efficiency due to this increase in pressure drop. If the additional pressure drop is not shown to have a big effect on the overall efficiency, then design B will be the design of choice.



(a) During max flow (WHX to CHX).



(b) During max flow (CHX to WHX).

Figure 9: Average pressure along the pulse tube for all three designs.

4 Conclusion and Future Work

The flow within the pulse tube of an existing SPTC has been numerically analysed. With the aid of the numerical simulations, a new inlet/outlet has been designed that will reduce flow mixing within the pulse tube. The next step will be to experimentally validate the results of the simulations.

Acknowledgments

The authors acknowledge support from the EPSRC under research project EP/N017013/1.

References

- [1] D. L. Gardner and G. W. Swift. Use of inertance in orifice pulse tube refrigerators. *Cryogenics*, 37(2):117–121, 1997.
- [2] P. C. T. De Boer. Performance of the inertance pulse tube. *Cryogenics*, 42(3):209–221, 2002.
- [3] S. Zhu and Y. Matsubara. Numerical method of inertance tube pulse tube refrigerator. *Cryogenics*, 44(9):649–660, 2004.
- [4] M. C. Brito and G. D. Peskett. Experimental analysis of free warm expander pulse tube. *Cryogenics*, 41(10):757–762, 2001.
- [5] S. Zhu and M. Nogawa. Pulse tube stirling machine with warm gas-driven displacer. *Cryogenics*, 50(5):320–330, 2010.
- [6] Y. Shi and S. Zhu. Experimental investigation of pulse tube refrigerator with displacer. *International Journal of Refrigeration*, 76:1–6, 2017.
- [7] Converge CFD. Converge CFD Website. [<https://convergecf.com/>], 2018.